Iranian Journal of Pharmaceutical Sciences
2025: 21 (1): 134- 144
https://journals.sbmu.ac.ir/IJPS

Research Article

Synthesis, Characterization, and Investigation of Performance of Fe-MOF and Fe-MOF/Fe_3O_4 in Adsorption and Release of Naproxen as a Non-steroid Anti-inflammatory Drug (NSAID)

Sayyde Shadi Hosseini[a], Seyed Ali Hosseini[a*], Mahin Broukanlou[a]

[a] *Department of Applied Chemistry, Faculty of Chemistry, Urmia University, 57561-51818, Urmia, Iran.*

Received: February 27, 2024 **Last Revision:** January 26, 2025 **Accepted:** February 22, 2025 **Available online:** April 26, 2025

Abstract

Developing materials with a high capacity for drug adsorption and slow-releasing properties is promising in drug delivery. Metal-organic frameworks (MOFs) are materials with high adsorption and desorption capacities. Therefore, they can be very effective in targeted drug therapy. In this study, two Fe-MIL101 samples with different synthesis times (24 and 48 hours) were synthesized by solvothermal method and used as a naproxen carrier for the first time. The samples were analyzed using BET, FT-IR, XRD, and FESEM structural analyses at the nanoscale. The pH_{pzc} of the Fe-MIL101 (48h) and Fe-MIL101/Fe_3O_4 was determined to be 3.3 and 3.5, respectively. The adsorption of the Naproxen on Fe-MIL-101/Fe_3O_4 followed the Freundlich adsorption isotherm (R^2=0.996), indicating the multilayer adsorption of Naproxen molecules on the carriers. The release of naproxen from carriers was investigated at a phosphate-buffered saline (PBS) with a pH of 7.4 (the pH of human blood). The variables of release time, carrier synthesis time, and pH of the environment were considered in this study. The most effective release was with Fe-MIL-101/Fe_3O_4 synthesized over 48 hours. This method followed the kinetic model of Korsmeyer-Peppas (R^2= 0.9843) with a release exponent (n) of 0.63, meaning that the naproxen release from MOFs follows the non-Fickian mechanism. To develop a magnetic and slow-releasing carrier, Fe-MIL-101/Fe_3O_4 was synthesized. The studies showed that naproxen release from Fe-MIL-101/Fe_3O_4 is slow and takes a long time. The n in Korsmeyer-Peppas mole for naproxen release from Fe-MIL-101/Fe_3O_4 was 0.886, indicating a case II transport mechanism for naproxen release with a constant release rate. The findings highlight the significant potential of Fe-MIL-101/Fe_3O_4 for enhancing targeted drug delivery, underscoring its importance in improving therapeutic outcomes.

Keywords: Drug Delivery; Metal-organic framework (MOF); Fe-MIL-101/Fe_3O_4; Korsmeyer-Peppas; non-Fickian mechanism; Naproxen.

1. Introduction

The routes of transferring various drugs inside bodily areas, organs, and cells are called drug delivery systems. Its typical objective is to enhance drug activity (drug therapy) and get rid of issues like inadequate solubility, drug buildup, low availability, poor biological distribution, and failure to choose or lessen the adverse

*** Corresponding Author**:
Seyed Ali Hosseini, Department of Applied Chemistry, Faculty of Chemistry, Urmia University, 57561-51818, Urmia, Iran.
E-mail: a.hosseini@urmia.ac.ir.

Cite this article as: Hosseini S.Sh., Hosseini S.A., Broukanlou M. Synthesis, Characterization, and Investigation of Performance of Fe-MOF and Fe-MOF/Fe3O4 in Adsorption and Release of Naproxen as a Non-steroid Anti-inflammatory Drug (NSAID). Iran. J. Pharm. Sci., 2025, 21 (1): 134- 144.

DOI: https://doi.org/10.22037/ijps.v21i1.44760

effects of medications properly. When a person first hears the name of a drug, tablets, capsules, and ampoules may be the only things that come to mind. However, there are many other ways to administer medications to the body. The medicine typically enters the body by two digestive methods: orally and by absorption into the blood through the gastrointestinal tract (injections, eye drops). Scientists are working to find ways to lessen and improve the side effects of pharmaceuticals because using these methods to introduce drugs also has side effects and harms in addition to the drug impact. Drug delivery methods were introduced after these efforts [1].

Drug delivery systems aim to deliver the medication to the desired site and keep the concentration within the therapeutic range. The medication dose should be administered over a predetermined period to have the most significant therapeutic benefit with the fewest side effects on healthy body tissue. Inflammation in the body and organs is an unfavorite state treated by anti-inflammatory drugs [2].

There are a variety of treatments for inflammation, but by far, the most common is the administration of non-steroidal anti-inflammatory drugs (NSAIDs). They are used for the treatment of both acute and chronic inflammation and are highly effective in the majority of cases. Over 40 different NSAIDs have been discovered, and they are often organized into multiple different classes based on structure and anticipated risk. Most NSAIDs are completely absorbed, have negligible first-pass hepatic metabolism, are tightly bound to serum proteins, and have small volumes of distribution. NSAIDs vary in their elimination half-lives, routes of administration, and tolerability profiles. Even though they are variable as a complete group, NSAIDs within a class tend to have similar characteristics. The most used NSAIDs in the world are Diclofenac, ibuprofen, naproxen, indomethacin, piroxicam, and ketoprofen. The different types of carriers, such as liposomes, polymer-based particles, clays, nanoparticles, and metal-organic frameworks (MOFs), have been studied in drug delivery [3].

Metal-organic frameworks (MOFs) are a novel porous material formed by coordinating metal ions with appropriate organic linkers. MOFs have garnered significant interest because of their large surface areas, crystalline structures, adjustable pore sizes, and functional properties. These characteristics make them suitable for gas storage, catalysis, separation, and drug delivery [4-6].

In a previous study, Senlin Wang et al. employed a novel pH-responsive Fe-MOF system for enhanced cancer treatment mediated by the Fenton reaction [7].

Malihe Pooresmaeil and co-workers developed a D-mannose functionalized MgAl-LDH/Fe-MOF nanocomposite as a new intelligent nanoplatforms for MTX and DOX co-drug delivery [8].

Yongmei Yang and co-workers employed Litchi-like Fe_3O_4@Fe-MOF capped with HAp gatekeepers for pH-triggered drug release and anticancer effect [9].

This work aimed to develop Fe-MIL 101 and a magnetic Fe-MIL 101/Fe_3O_4 composite as naproxen nanocarrier for studying naproxen release from them in an *in-vitro* system. Naproxen is used to treat body inflammation, such as bone inflammation. The isotherms of naproxen adsorption on the carrier were studied. Then, the kinetic and mechanism for releasing naproxen from the carriers were studied. The effects of pH on naproxen release and Fe_3O_4 incorporation on Fe-MIL 101 on naproxen release rate to get a slow-releasing carrier were studied.

2. Materials and Methods

2.1. Synthesis of Fe-MIL101 carrier

Two samples of Fe-MOF were synthesized using the solvothermal synthesis method. The synthesis conditions for the two samples were the same, but the synthesis times were different. Typically, 20 mL of DMF was used to dissolve 4.2 g of iron(II) chloride. 1.03 g of terephthalic acid was added, then the solution was placed in an ultrasonic bath for 30 minutes. The solution was poured into a Teflon-lined autoclave and heated in an oven at 100°C. For the first sample, the synthesis time was 24 hours, and for another, 48 hours. Finally, the precipitate of each batch was filtered and cleaned with ethanol [10]. Hereafter, they were nominated as Fe-MIL101 (24 h) and Fe-MIL101 (48 h).

2.2. Synthesis of Fe_3O_4 nanoparticles

50 ml of ethanol was added to 0.01 M of iron chloride ($FeCl_3.6H_2O$) and 0.02 M of iron chloride ($FeCl_2.4H_2O$). Then, 3 M sodium hydroxide solution was added dropwise and stirred until the pH equaled 10. After

stirring for 12 hours, a few drops of ethylene glycol (surfactant) were added to the mixture. Then, the sediment was cleaned with ethanol and distilled water to obtain a pH of 7. Finally, the solution was dried under a vacuum at 60 °C.

2.3. Preparation of Fe-MOF/Fe_3O_4 composite

50 mL of distilled water and 50 mL of ethanol were added to 0.1 g of Fe-MIL101 carrier and 0.1 g of Fe_3O_4. After stirring for one hour, the mixture was strained, washed several times with water and ethanol by a vacuum filter, and dried at 150 °C.

2.4. Characterization of the carrier

The XRD pattern of the MOF carriers was recorded on a Siemens D500 diffractometer (Germany) with Cu Kα. Fourier-transform infrared (FTIR) spectroscopy was used to study the presence of functional groups and molecular vibrations by a Bruker Tensor 27 spectrophotometer (Germany). The morphology of the samples was investigated by A FE-SEM ZEISS (Sigma model). The surface area of the drug carriers was evaluated through N_2 adsorption-desorption isotherms and Brunauer-Emmett-Teller (BET) plots generated using a Belsorp Mini II instrument (Japan) at 77 K.

2.5. The drug loading on the Fe-MIL 101 carrier

0.1 g of the selected carrier was added to 200 ml of 20 ppm naproxen solution at 25 ℃ and stirred for one hour. Then, nano filter paper filters the beaker contents (sediment containing brick paint). Finally, the absorption of the sub-filter solution containing naproxen was stabilized at a certain value. Then, it was dried for the next step, investigating the drug release from the sediment surface. The experiments were repeated several times on the carrier with different drug concentrations at a constant temperature to check the consistency and accuracy of the data. The efficiency of drug entrapment and the capacity for drug loading were determined using specific equations. Where W_0 is the starting amount of naproxen(mg), W_f is the amount of naproxen (mg) present in the final solution, W_e are the amount of the drug (mg) incorporated into the carriers, W_{ads} is the amount of the carrier (g) [11, 12].

$$\text{The efficiency of drug entrapment} = \frac{W_0 - W_f}{W_f} \times 100 \quad (1)$$

$$\text{Capacity for drug loading} = \frac{W_e}{W_{ads}} \quad (2)$$

2.6. Naproxen release from Fe-MIL 101 carrier

The release experiments were carried out using phosphate buffer solutions (PBS) with a pH value of 7.4 (representing the pH of human blood). The Fe-MIL 101/naproxen powder was poured inside a dialysis tubing cellulose membrane and placed in 100 ml phosphate buffer (PBS). Periodically, a specific volume of PBS (4ml) was withdrawn from the Naproxen release medium and replaced with fresh PBS. The concentration of Naproxen in the PBS buffer was determined using a UV-visible spectrophotometer and the calibration plot for naproxen to assess the released concentration of naproxen. The calibration curve of the naproxen is presented in **Figure 1**. The percentage of released naproxen from the carrier can be determined using Eq.3. In this equation, W_r represents the total amount of naproxen that has been released (in milligrams), while W_e indicates the amount of naproxen initially loaded onto the carrier (in milligrams) [12].

$$\text{The percentage of naproxen released} = \frac{W_r}{W_e} \times 100 \quad (3)$$

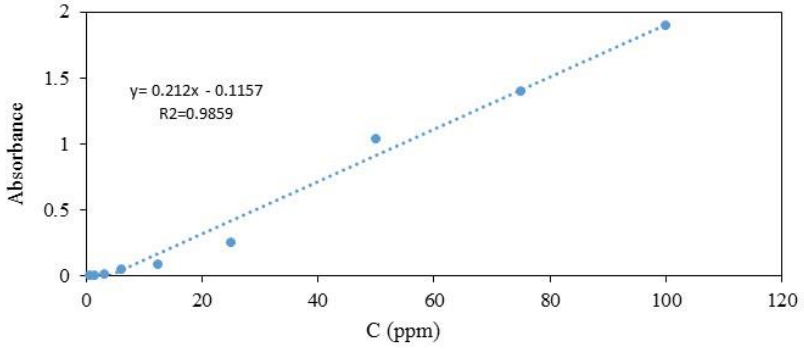

Figure1. Calibration plot of Naproxen

2.7. Kinetic studies

Kinetic models describe the overall drug release from the amount of drug absorbed. Quantitative and qualitative changes in the kinetic formulation can affect drug release in vivo system. Developing equipment that facilitates product development while reducing the need for biological studies has always been desirable. Kinetic studies of drug release were done to investigate the release of naproxen loaded in the carriers. The concentration of the released naproxen during different times was measured to study the kinetics of naproxen release. The data were plotted versus times and fitted with different kinetic models. Several models, including zero-order, first-order, second-order, Higuchi, and Korsmeyer-Peppas models, describe drug release kinetics from various matrices.

3. Results and discussion

3.1. FT-IR Study

The FTIR spectra of the naproxen, Fe-MIL101, and magnetic Fe-MIL101, Fe-MIL101/naproxen, and magnetic Fe-MIL101/naproxen. **Figure 2a** shows the FTIR spectrum of Naproxen. The peaks at 700-1000 cm^{-1} correspond to C-H bending vibrations. The peak around 1167 cm^{-1} corresponds to CH_3-O, and those around 1500 and 1717 cm^{-1} correspond to C=C of aromatic rings and carbonyl groups of the carboxylate (O-C=O), respectively. The peak at 1100 cm^{-1} indicates the O-C stretching vibrations of the methoxy group, and those at 2937 cm^{-1} and 3003 cm^{-1} are ascribed to the C-H stretching at aliphatic and aromatics, respectively. The peak at 3500 cm^{-1} is related to O-H stretching vibrations. Similar peaks are observed in the samples of **2c** and 2e. These peaks at the spectra of **Figure 2b** and **2d** indicate the ligands of MOF structure, i.e., Terephthalate, and the peak at all spectra around 500 cm^{-1} corresponds to the Fe-O vibration at MOFs [13-16].

3.2. FE-SEM analysis

The FESEM images of the carrier synthesized at two different times (24 and 48 h) are shown in **Figure 3**. The images of Fe-SEM (24 h) are shown in **Figure 3a.** It is evident from FE-SEM images that the particle shapes of the synthesized Fe-MIL101 are rhombic. The morphology and particle shape of Fe-MIL101 (48 h) in **Figure 3b** are similar to those of Fe-MIL101 (24h), but more porosity is observed in particles of **Figure 3(b)**. The morphologies of the synthesized Fe_MIL101 carriers correspond with the morphology of those reported in the literature [17, 18]. Therefore, the morphology and particle shape of the samples prove the formation of Fe-MIL-101.

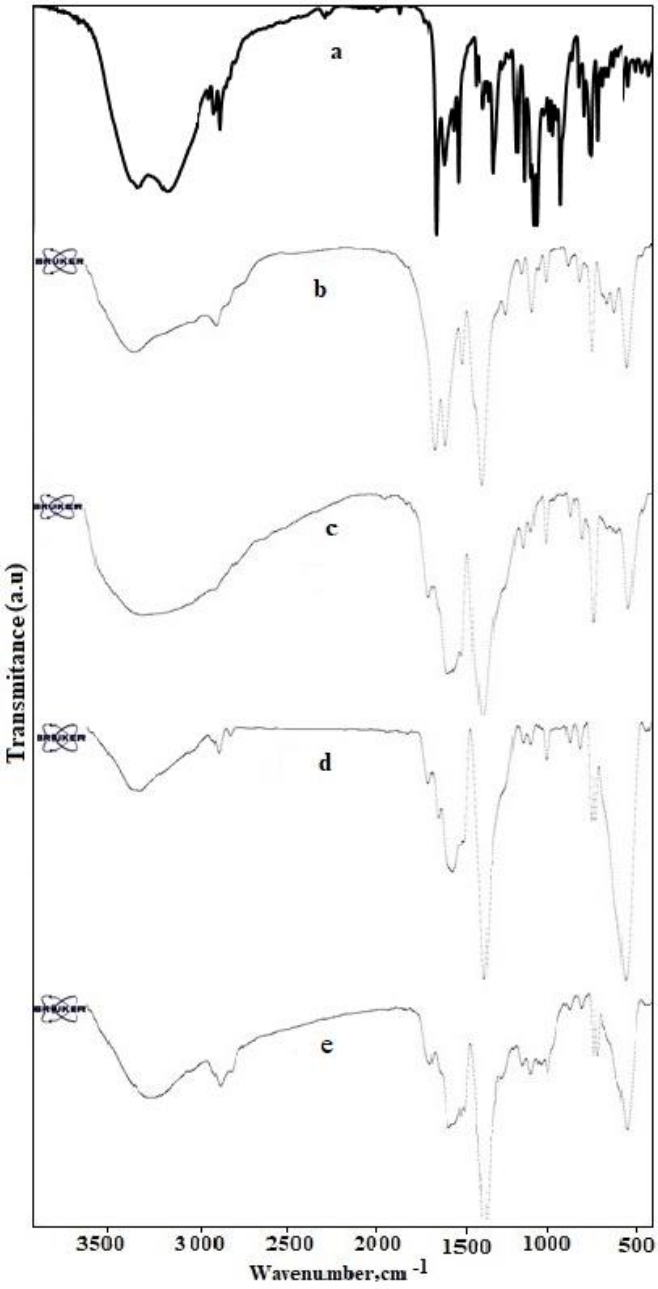

Figure 2. FTIR of Naproxen (a), Fe-MOF (b), Fe-MOF/Naproxen (c), Fe-MOF/Fe_3O_4 (d), and Fe-MOF/Fe_3O_4 -Naproxen (e).

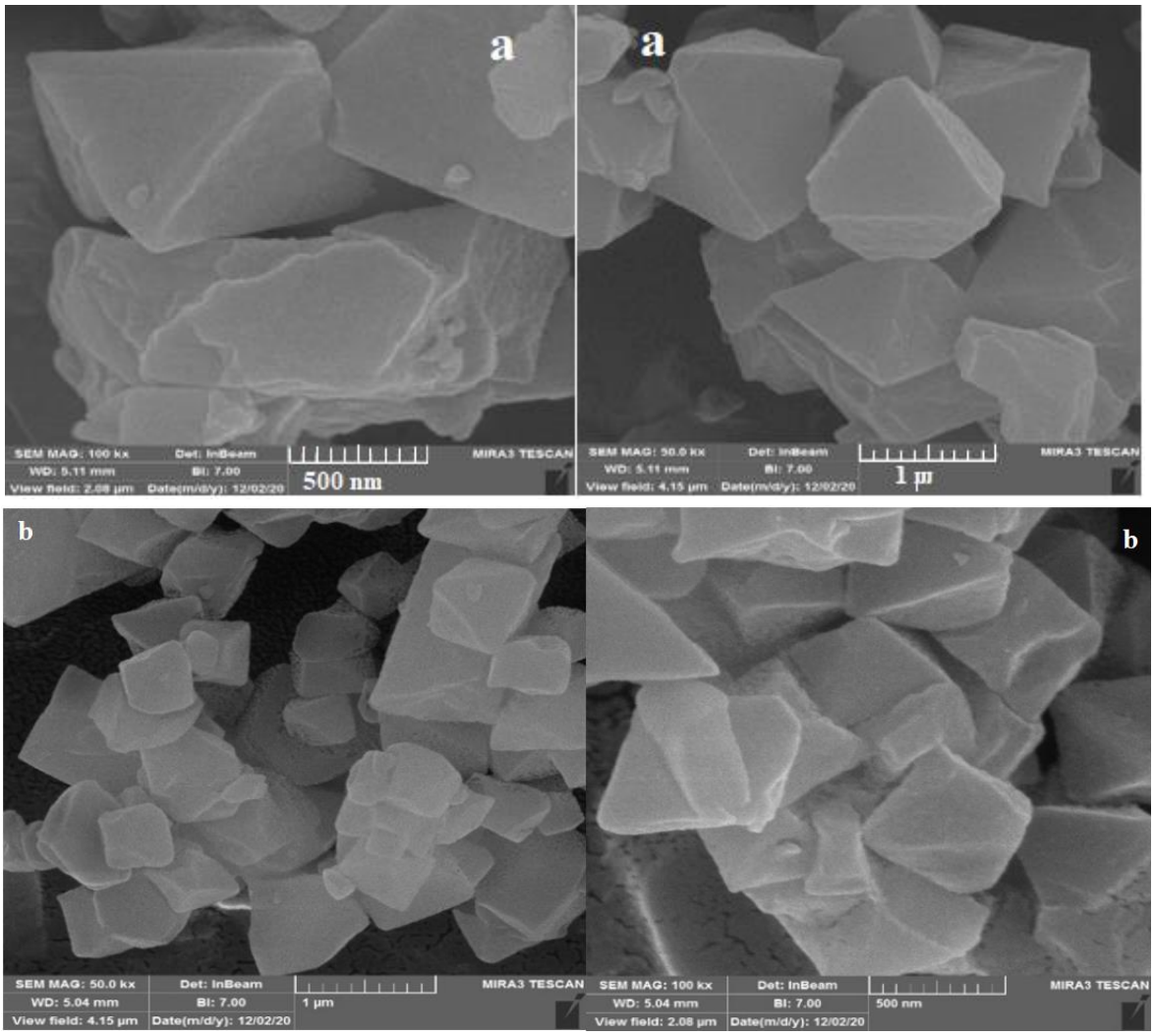

Figure 3. FE-SEM for (a) Fe_MIL101 (24h) and (b) Fe_MIL101 (48h)

3.3. XRD results

The X-ray diffraction pattern of the two samples (24 and 48 h.) shown in **Figure 4** indicates that an organic-metallic structure has formed. The peak indicates the MOF structure at 36.5, 35, 34.2, 30.9, 27.6, 22.25, 21.39, 18.99, 18.08, 14.8, 11.9, and 9.2, consistent with the literature [19]. The peaks are not so sharp, meaning that the time for the formation of MOF was low, and it is also possible that the unreacted A comparison of the samples' X-ray diffraction patterns for Fe_MIL101 samples with the synthesized times of 24 and 48 hours indicates the similar patterns but a difference in the peak intensities. The intensity of peaks at the pattern of MOF (48 h.) is higher, indicating that the growth rate of the organic-metallic structure accelerates with longer synthesis times [20-22].

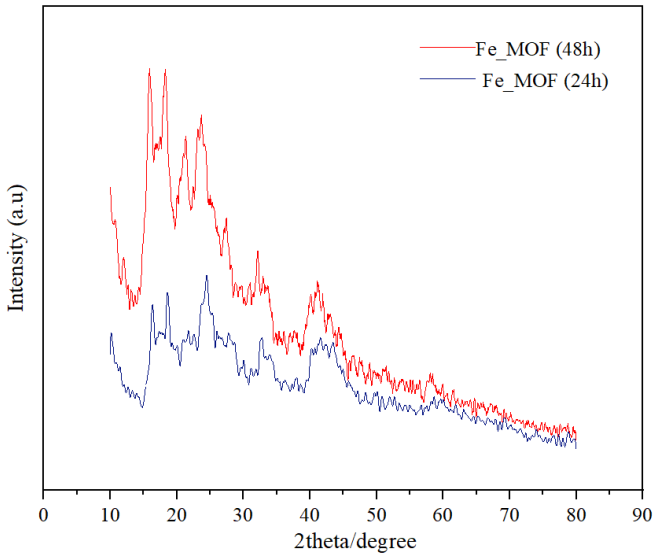

Figure 4. XRD for Fe_MIL101 carriers, synthesized during 24h and 48 h

3.4. BET analysis

Figure 5 shows the microstructural properties of the average capillary structure of Fe-MIL101 (24 and 48 h.) through nitrogen adsorption-desorption isotherm (BET) studies.

The adsorption-desorption curves in **Figures 5a** and **5b** correspond to the type II isotherm, indicating the presence of a medium capillary type in the MOF carriers. Isotherm II derives from the Langmuir model, indicating multilayered adsorption [23]. In the BET equation for Fe-MIL101 (24 h.), C equals 30.79, whereas it is 104.63 for Fe-MIL101 (48 h.). The BET isotherm resulted in a specific surface area of 44.99 and 95.52 m^2/g for Fe-MIL101 (24 h.) and Fe-MIL101 (48 h.), respectively. The increasing synthesis time increased the surface area of the MOF, which is attributed to the growth of the MOF framework. However, we expected a higher surface area for Fe-MIL101 (24 h.), but some papers reported some MOFs with low surface area. For example, Tran et al. reported the synthesis of Fe-MOF with a surface area of 32 m^2/g [24]. The surface area of the Fe-MIL-101 (24h)/Fe_3O_4 and Fe-MIL-101 (48 h.) decreased to 39.65 and 90.23 m^2/g due to the loading of Fe_3O_4 particles on MOF.

3.5. Determination of pHpzc of Fe-MIL101 and Fe-MIL101/Fe_3O_4

pH of the solution is one of the effective factors on surface charges of the adsorbent (herein drug carrier) [25]. Determining the pH where the surface charges become zero is important. This pH is called pHpzc. The pHpzc was determined by the pH drift method reported in the literature [24, 26]. Briefly, several solutions containing 0.01 $mol.L^{-1}$ NaCl were supplied. The initial pH of the solutions was adjusted to a value between 2 and 10 using 0.01 $mol.L^{-1}$ HCl or NaOH. 20 mg adsorbent was added to the solutions. The solutions containing adsorbent were kept for 24 h. to reach equilibrium. Then, the pH of the solutions (pH_f) was recorded. The plot of pH_f versus pH_i was plotted. The pH at which pH_i crossovered the (pH_f) was called the pH_{PZC}. The pH_{PZC} for Fe-MIL101 and Fe-MIL101/Fe_3O_4 was determined at 3.3 and 3.5, respectively.

3.6. Investigation of drug release of naproxen

Three pH levels were considered, 4.8, 6.8, and 7.4, to investigate the effect of pH on the release of naproxen. The findings showed that the release of naproxen increased at an alkaline pH. Since this work's objective was to study naproxen release in biological pH, the phosphate-buffered saline (PBS(with pH = 7.4) was selected for the studies. It simulates the biological conditions such as human blood. The release of naproxen from naproxen loaded on Fe-MIL 101 (24 h.), Fe-MIL 101 (48 h.), and Fe-MIL 101/Fe_3O_4 was studied in a Phosphate-buffered saline (PBS) with pH = 7.4, simulating the human blood conditions). The results are shown in **Figure 6**. It is observed in the figure that the release rate of naproxen from

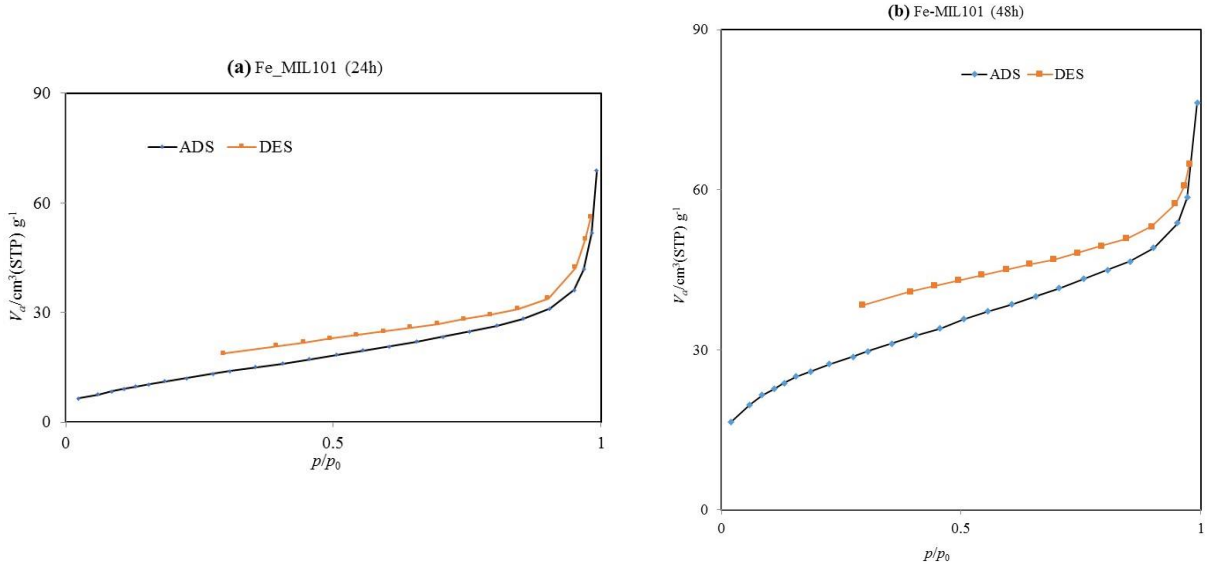

Figure 5. BET for Fe_MIL101 with synthesis times of (a): 24h and (b): 48 h

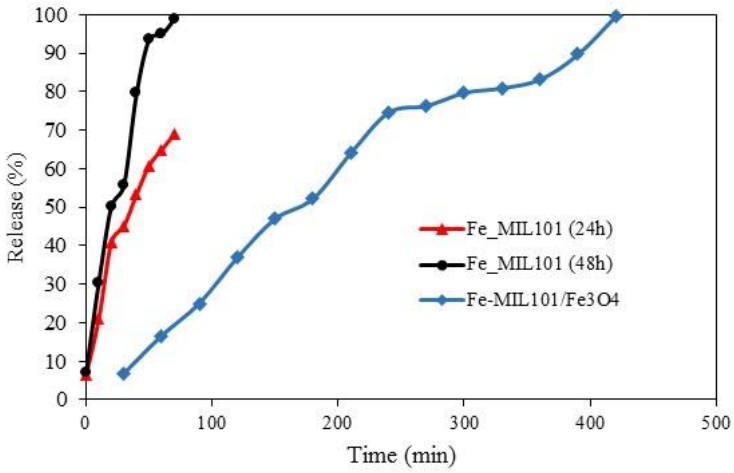

Figure 6. Release percentage of naproxen from Fe-MIL 101 (synthesized in 24 hours), Fe-MIL 101 carrier synthesized in 48 hours, and Fe-MIL 101/Fe_3O_4

3.7. Kinetic models in drug delivery

The drug release from formulations is crucial, particularly in modified and immediate-release dosage forms. Various factors such as the physicochemical properties of drugs, excipients, dosage form design, manufacturing process variables, and design influence drug release from dosage forms. It is imperative to investigate the drug release pattern from dosage forms as it determines the efficacy of the dosage form. Several models aid in understanding the release pattern, thereby enabling the design of an effective formulation [27, 28]. In this section, some conventional kinetic models for drug delivery were considered. The models were applied to all carriers; the results are shown in **Table 1**. Herein, the models are described briefly [27, 28].

Zero-order model

Ideal drug delivery systems are designed to exhibit zero-order kinetics, maintaining a stable drug concentration in the bloodstream throughout the release process. This concept can be mathematically represented by Equation (4). Where, Q_t indicates the quantity of drug released into the medium at time t, Q_0 represents the initial concentration (typically set to zero), and K_0 denotes the zero-order release constant.

$$Q_t = Q_0 + K_0 t \quad (4)$$

First-Order Model

The first-order kinetics model establishes a linear relationship between the rate of change in concentration and the concentration gradient of the drug between the surface of the carrier and the surrounding liquid. This relationship can be simplified to Equation (5), where C is the concentration of the drug released at time t, C_0 is its initial concentration, and K is the first-order rate constant.

$$\log C = \log C_0 - KT/2.303 \quad (5)$$

Higuchi Model

Higuchi developed a mathematical model for drug release from an insoluble porous matrix based on Fick's laws of diffusion, expressed in Equation (6). In this equation, the total amount of drug released at time t (Q_t) is proportional to the square root of time, with K_H representing Higuchi's dissolution constant.

$$Q_t = K_H\, t^{1/2} \quad (6)$$

Korsmeyer–Peppas Model

Introduced in 1983, the Korsmeyer–Peppas model describes drug release from polymeric substrates where diffusion is the primary mechanism. The fundamental equation for this model is given as Equation (7), where f represents the fraction of drug released at time t, M_t is the amount of drug released at that time, M_∞ is the total amount of drug in equilibrium, K is a constant that reflects the structural and geometric properties of the carrier, and n is an exponent that characterizes various release mechanisms [27, 28].

$$f = M_t / M_\infty = Kt^n \quad (7)$$

Table 1. Investigating kinetic models for naproxen release from the carriers

Carrier	Zero order		First order		Second order		Higuchi-model		Korsmeyer-Peppas		
	k	R^2	k	R^2	k	R^2	k	R^2	k	n	R^2
Fe_MIL101 (24h)	0.102	0.92	0.025	0.73	0.012	0.51	0.092	0.96	0.694	0.59	0.96
Fe_MIL101 (48h)	0.128	0.94	0.027	0.75	0.013	0.48	1.15	0.97	1.45	0.63	0.97
Fe_MIL101 /Fe_3O_4	0.027	0.95	0.004	0.82	0.017	0.46	0.74	0.98	0.06	0.886	0.98

Table 1 shows that Korsmeyer Peppa's model could fit the experimental data with a high correlation among all models. The coefficient of determination (R^2) for this model was the highest. So, it resulted that the release of naproxen over Fe_MIL101 (24h), Fe_MIL101 (48h), and Fe_MIL101 /Fe_3O_4 carriers follows the Korsmeyer Peppa's model. Maghsoudi et al. reported that the Korsmeyer Peppa's model is the best model for releasing Doxorubicin from DOX-encapsulated magnetic liposome@PEG [28]. Yucheng Shi et al. studied the kinetic release of Doxorubicin from Fe-MIL101 and resulted in Korsmeyer Peppa's model as the most suitable model for describing DOX-releasing kinetic [29].

As stated before, the release exponent(n) at Korsmeyer Peppa's model indicates the release rate mechanism. According to the literature [27-29], 0.45 < n < 0.89 indicates that the mechanism of the drug follows the anomalous (non-Fickian) diffusion. In the Fe_MIL101 /Fe_3O_4 carrier, the n is 0.883, whereas the n for Fe_MIL101 (24h) and Fe_MIL101 (48h) is 0.59 and 0.63, respectively. Since the n=0.886 is close to 0.89, the Zero order release (Case II transport) indicates a slow-releasing rate [30]. The results of naproxen release from different carriers (**Figure 6**) indicate that the release from Fe_MIL101 /Fe_3O_4 is slower and takes a long time. The incorporation of Fe_3O_4 on Fe_MIL101 led to the formation of a slow-releasing carrier for naproxen.

3.8. Isotherm survey results

The relationship between the quantity of adsorbate on an adsorbent and the equilibrium concentrations of the adsorbate in the solution can be elucidated through adsorption isotherms. These isotherms reveal how adsorbate molecules diffuse between the liquid and solid phases when the adsorption process approaches equilibrium [31]. Two isotherms, Langmuir and Freundlich [32-34], were studied to investigate the surface of the Fe-MIL 101 carrier. The results are shown in **Tables 2** and **3**.

According to the plots and data obtained, the isotherm for the Fe-MIL101 carrier synthesized in 24 hours follows the Freundlich model and is physically adsorbed, according to research by Yucheng Shi et al. [29], Yang et al. [34], Pofang et al. [35] and Hamedi et al. [36].

Table 2. Freundlich and Langmuir isotherms for 0.1 g of Fe-MIL carrier synthesized in 24 hours

Isotherms	Equations	R^2
Freundlich	$\log q_e = \log k_f + \frac{1}{n}\log C_e$ K_F=1.220 (mg. g^{-1}) 1/n= 0.363 n = 2.748 ($L.mg^{-1}$)	R^2=0.942
Langmuir	$\frac{C_e}{q_e} = \frac{C_e}{q_{max}} + \frac{1}{K_L * q_{max}}$ q_m=0.0189(mg. g^{-1}) K_L= 5.0505($L.mg^{-1}$)	R^2=0.699

Table 3. Freundlich and Langmuir isotherms for 0.1 g of Fe-MIL carrier synthesized in 48 hours

Isotherms	Equations	R^2
Freundlich	$\log q_e = \log k_f + \frac{1}{n}\log C_e$ K_F=1.056 (mg.g^{-1}) 1/n= 0.415 n = 2.409 (L.mg^{-1})	R^2=0.996
Langmuir	$\frac{C_e}{q_e} = \frac{C_e}{q_{max}} + \frac{1}{K_L * q_{max}}$ q_m=0.075(mg.g^{-1}) K_L= 0.172 (L.mg^{-1})	R^2=0.9846

4. Conclusions

An important goal of drug delivery is to obtain a constant release rate for a prolonged time. For the first time, two Fe-MIL101 carriers were synthesized at two different synthesis times (24 and 48 hours) and used as a carrier for naproxen. The drug was successfully loaded onto the Fe-MIL101 carrier, and its release was investigated at pH 7.4. The kinetic studies for naproxen release from both Fe-MIL101 carriers followed the non-Fickian diffusion mechanism. The variables of release time, carrier synthesis time, and pH of the environment were considered. The most effective release resulted in the case of magnetized Fe-MIL101 (48 h), following the kinetic model of Korsmeyer-Peppas (R^2= 0.9843) and the Freundlich adsorption isotherm (R^2=0.996). The incorporation of Fe_3O_4 into Fe-MIL101 developed a magnetic carrier that prolonged the release time. The release exponent of ~0.89 in the kinetic model of Korsmeyer-Peppas confirmed that the transport rates are independent of time (Case II transport) and developed a slow-releasing carrier for naproxen. Magnetic Fe-MOFs such as Fe_MIL101/Fe_3O_4 could be an alternative carrier for the magnotherapy of cancers.

Athors Orcid numbers:

Sayyde Shadi Hosseini: 0009-0002-2656-0033
Seyed Ali Hosseini: 0000-0002-3969-3241
Mahin Broukanlou: 0009-0008-0876-0406

Using artificial intelligence chatbots

There was no use of artificial intelligence in the making of this article.

References

1. Shahifar, A., Bagheri, H., & Namnabat, S. Synthesis and Evaluation of a Polycaprolactone-methoxy-Polyethyleneglycol Copolymer Nano-system for Curcumin and Tacrolimus Release: Drug Delivery Nano-system. *Iranian J. Pharm. Scientists (2023) 19*(4):304–313.
2. Sadeghi, M., Chegini, R., khafaei, M., Sabbagh ziarani, F., & Zafari, F. Association of Atorvastatin with GDF9 and BMP15 Expression and in vitro Maturation of Mouse Oocytes: Atorvastatin GDF9 and BMP15 Expression and Mouse Oocytes. Iranian J. Pharm. Scientists (2023) 19(3): 188–193.
3. Brune K, Patrignani P., New insights into the use of currently available non-steroidal anti-inflammatory drugs. J. pain Res. (2015) 8:105-18.
4. Mishra P, Edubilli S, Uppara HP, Mandal B, Gumma S. Effect of adsorbent history on adsorption characteristics of MIL-53 (Al) metal organic framework. Langmuir (2013) 29(39):12162-7.
5. Horcajada P, Serre C, Vallet- Regí M, Sebban M, Taulelle F, Férey G. Metal–organic frameworks as efficient materials for drug delivery. Angewandte chemie. (2006)118(36):6120-4.
6. Song X, Nong L, Zhang M, Liu J. Efficient removal of As (Ⅲ) by a La/Fe composite membrane filter: The composite form of La, the dynamic adsorption and adaptability. J. Environ Chem. Eng. (2024) 12(4):113056.
7. Wang S, Wu H, Sun K, Hu J, Chen F, Liu W, Chen J, Sun B, Hossain AM. A novel pH-responsive Fe-MOF system for enhanced cancer treatment mediated by the Fenton reaction. New J .Chem. (2021) 45(6):3271-9.
8. Pooresmaeil M, Namazi H. D-mannose functionalized MgAl-LDH/Fe-MOF nanocomposite as a new intelligent

nanoplatform for MTX and DOX co-drug delivery. Int. J. Pharm. (2022) 625:122112.
9. Yang Y, Xia F, Yang Y, Gong B, Xie A, Shen Y, Zhu M. Litchi-like Fe 3 O 4@ Fe-MOF capped with HAp gatekeepers for pH-triggered drug release and anticancer effect. J Mater Chem B (2017) 5(43):8600-6.
10. Cao J, Li X, Wang X, Li K, Liu Y, Tian H. Surface PEGylation of MIL-101 (Fe) nanoparticles for co-delivery of radioprotective agents. Chem. Eng. J. (2020) 384:123363.
11. Dhakar RC, Maurya SD, Sagar BP, Bhagat S, Prajapati SK, Jain CP. Variables influencing the drug entrapment efficiency of microspheres: A pharmaceutical review. Der Pharm. Lett. (2010) 2(5):102-16.
12. Broukanlou M, Hosseini S.A, Pazhang Y, ZSM-5/PEG/DOX nanocarrier for pH-responsive doxorubicin release: Kinetic, isothermal, and cytotoxic studies, Micropor. Mesopor. Mater (2025) 387: 113531.
13. Amdeha E, Mohamed RS. A green synthesized recyclable ZnO/MIL-101 (Fe) for Rhodamine B dye removal via adsorption and photo-degradation under UV and visible light irradiation. Environ. Technol. (2021) 42(6):842-59.
14. Xie Q, Li Y, Lv Z, Zhou H, Yang X, Chen J, Guo H. Effective adsorption and removal of phosphate from aqueous solutions and eutrophic water by Fe-based MOFs of MIL-101. Sci. Rep. (2017) 7(1):3316.
15. Mehta R, Chawla A, Sharma P, Pawar P. Formulation and in vitro evaluation of Eudragit S-100 coated naproxen matrix tablets for colon-targeted drug delivery system. J. Adv. Pharm. Technol. Res (2013) 4(1):31.
16. Mohammadzadeh D., Hosseini S.A., Removal of Dibenzothiophene from Liquid Fuels by Photocatalytic Desulfurization over Zn- Terephthalate Complex: A Process Modelling and Optimization by Response Surface Methodology, ChemistrySelect (2023) 8: e202302400
17. Li, L., MOFzyme: Enzyme Mimics of Fe/Fe-MIL-101. Journal of Biosciences and Medicines (2019) 7(05) 213.
18. Nikou, M. and A. Samadi-Maybodi, Application of chemometrics into simultaneous monitoring removal efficiency of two food dyes by an amine-functionalized metal–organic framework. J. Iranian Chem. Soc. (2020) 1-23.
19. Amdeha E., Mohamed R.S., A green synthesized recyclable ZnO/MIL-101(Fe) for Rhodamine B dye removal via adsorption and photo-degradation under UV and visible light irradiation, Environ. Technol. (2021) 42: 842-859
20. He L, Dong Y, Zheng Y, Jia Q, Shan S, Zhang Y. A novel magnetic MIL-101 (Fe)/TiO2 composite for photodegradation of tetracycline under solar light. J. Hazard. Mater.(2019) 361:85-94.
21. Thanh HT, Phuong TT, Le Hang PT, Toan TT, Tuyen TN, Mau TX, Khieu DQ. Comparative study of Pb (II) adsorption onto MIL–101 and Fe–MIL–101 from aqueous solutions. J. Environ. Chem. Eng. (2018) 6(4):4093-102.
22. Karami K, Beram SM, Siadatnasab F, Bayat P, Ramezanpour A. An investigation on MIL-101 Fe/PANI/Pd nanohybrid as a novel photocatalyst based on MIL-101 (Fe) metal-organic frameworks removing methylene blue dye. J. Mol. Struct. (2021) 1231:130007.
23. Lorenz M, Paganini C, Storti G, Morbidelli M. Macroporous polymer–protein hybrid materials for antibody purification by combination of reactive gelation and click-chemistry. Mater. (2019) 12(10):1580.
24. Tran T.K.N, Khanh Phan C.P., Chau H.D., Do T.S., Co-doped Fe-MOF bimetallic organic framework applied as adsorbent to treat methylene blue dye in wastewater, Mater. Today (2024) In press.
25. Ebrahimi F., Nabavi S.R., Omrani A., Fabrication of PAN/PA6//rGO-TiO2 electrospun nanofibers membrane with self-cleaning performance under visible light, J Appl Polym Sci. (2022) 140: e53523
26. Ebrahimi F., Nabavi S.R., Omrani A., Fabrication of hydrophilic hierarchical PAN/SiO2 nanofibers by electrospray assisted electrospinning for efficient removal of cationic dyes, Environ. Technol. Innov. (2022) 25: 102258
27. Paarakh MP, Jose PA, Setty CM, Peterchristoper GV. Release kinetics–concepts and applications. Int. J. Pharm. Res. Technol. (2018) 8(1):12-20.
28. Maghsoudi S., Hosseini S.A., Soraya H., Roosta Y., Mohammadzadeh A., Development of doxorubicin-encapsulated magnetic liposome@PEG for treatment of breast cancer in BALB/c mice, Drug Deliv. and Transl. Res. (2023) 13: 2589–2603.
29. Shi Y, Wang Y, Zhu J, Liu W, Khan MZ, Liu X. Molecularly imprinting polymers (MIP) based on nitrogen doped carbon dots and mIL-101 (Fe) for doxorubicin hydrochloride delivery. Nanomater. (2020) 23:10(9):1655.
30. Ahmed L., Atif R., Eldeen T.S., Yahya I., Omara A., Eltayeb M., Study the Using of Nanoparticles as Drug Delivery System Based on Mathematical Models for Controlled Release, Int. J. Latest Technol. Eng. Manag. Appl. Sci. (2019) 8: 52-56.
31. PourShaban M, Moniri E, Safaeijavan R, Panahi HA. Kinetics, isotherm and adsorption mechanism studies of letrozole loaded modified and biosynthesized silver

nanoparticles as a drug delivery system: comparison of nonlinear and linear analysis. Korean Chem. Eng. Res. (2021) 59(4):493-502.

32. Chung HK, Kim WH, Park J, Cho J, Jeong TY, Park PK. Application of Langmuir and Freundlich isotherms to predict adsorbate removal efficiency or required amount of adsorbent. J. Ind. Eng. Chem. (2015) 28:241-6.
33. Firdaus M, Wahyuningsih S, Nugrahaningtyas KD, Hidayat Y. Derivation and constants determination of the Freundlich and (fractal) Langmuir adsorption isotherms from kinetics. IOP Conference Series: Materials Science and Engineering (2018) 333: 012010.
34. Yang Y, Zheng Z, Ji W, Xu J, Zhang X. Insights to perfluorooctanoic acid adsorption micro-mechanism over Fe-based metal organic frameworks: Combining computational calculation with response surface methodology. J. Hazard. Mater. (2020) 395:122686.
35. Feng P, Chen J, Fan C, Huang G, Yu Y, Wu J, Lin B. An eco-friendly MIL-101@ CMCS double-coated dinotefuran for long-acting active release and sustainable pest control. J. Clean Prod. (2020) 265:121851.
36. Hamedi A, Zarandi MB, Nateghi MR. Highly efficient removal of dye pollutants by MIL-101 (Fe) metal-organic framework loaded magnetic particles mediated by Poly L-Dopa. *J. Environ. Chem. Eng.* (2019) 7(1):102882.